Arabian Journal of Chemistry (2020) **13**, 6649–6661

King Saud University

Arabian Journal of Chemistry

www.ksu.edu.sa
www.sciencedirect.com

ORIGINAL ARTICLE

Glycidyl ether of naturally occurring sesamol in the synthesis of mussel-inspired polymers

Shaikh A. Ali [a,*], **Mouheddin T. Alhaffar** [a], **Mohammad N. Akhtar** [b]

[a] *Chemistry Department, King Fahd University of Petroleum & Minerals, Dhahran 31261, Saudi Arabia*
[b] *Center for Refining and Petrochemicals, RI, King Fahd University of Petroleum & Minerals, Dhahran 31261, Saudi Arabia*

Received 30 April 2020; accepted 16 June 2020
Available online 25 June 2020

KEYWORDS

Sesamol;
Allyl glycidyl ether;
Sesamol glycidyl ether;
Epoxy polymerization;
Triisobutylaluminium;
Thiol-ene reaction

Abstract The objective of this work is to synthesize the mussel-mimicking ionic polymers bearing electron-rich 1,3,4-triphenoxy motifs of naturally occurring sesamol [3,4-(methylenedioxy)phenol] **I**. To our knowledge, the work would represent, for the first time, the ring-opening reaction of epoxide built upon the triphenoxy motifs of hydroxyhydroquinone. Sesamol **I** upon O-alkylation using epibromohydrin has been converted to its epoxy monomer **II** in 77% yield. Monomer **II** under ring-opening polymerization using basic Bu_4NOH and Bu_4NF as well as by Lewis acid initiator/catalyst $MePh_3PBr/{}^{i}Bu_3Al$ led to polyether **III** in 80–99% yields. Monomer **II** and allyl glycidyl ether (i.e. allyl 2,3-epoxypropyl ether) **IV** upon polymerization gave random copolymer **V** of number average molar mass of 9570 g mol^{-1}, which upon thiol-ene reaction with $HSCH_2CH_2NH_3^+Cl^-$ and $HSCH_2$-CO_2H afforded cationic ($\hat{}\hat{}\hat{}NH_3^+$) **VI** and anionic ($\hat{}\hat{}\hat{}CO_2^-$) **VII** copolymers, respectively. For facile deprotection, the methylenedioxy (—OCH_2O—) motifs in **VI** was activated by its conversion to labile acetoxymethylenedioxy [—OCH(OAc)O—] unit to obtain **VIII** in 80% yields. The pendant allyl groups in **VIII** upon elaboration *via* thiol-ene reaction using cysteamine hydrochloride and subsequent hydrolysis of [—OCH(OAc)O—] under a mild condition led to a mussel-inspired cationic copolymer **IX** (78%) having catechol motifs-embedded pendants of 3,4-dihydroxyphenoxy groups.

1. Introduction

Many synthetic nano-structured epoxy-based adhesives have been developed for surface coating (Jouyandeh et al., 2019; Ahmadi, 2019; Jouyandeh et al., 2018a, b). Synthetic adhesive polymers quite often do not perform well in aquatic environment owing to deleterious effects of hydrolysis, moisture-wicking, swelling, etc. (Comyn, 1981; Lee et al., 2011). Holdfast of marine mussels secrets different moisture-resistant adhesive proteins, containing ≈1-28 mol% of 3,4-dihydroxyphenyl-L-alanine (L-DOPA) which stick rapidly and strongly to solid surfaces in the turbulent sea. (Comyn, 1981). The catecholic functionalities (i.e. 3,4-dihydroxyphenyl) in DOPA-decorated proteins provide strong covalent interfacial interactions. This has led researchers to mimic the adhesive chemistry practiced by the mussels. Several

* Corresponding author.
E-mail address: shaikh@kfupm.edu.sa (S.A. Ali).
Peer review under responsibility of King Saud University.

Production and hosting by Elsevier

https://doi.org/10.1016/j.arabjc.2020.06.020
1878-5352

reviews articulate the biomimetic design incorporating catechol-functional motifs to replicate the natural adhesive systems for various applications including anti-biofouling and drug delivery (Basiri et al., 2018; Kaushik et al., 2015; Wang et al., 2018; Zhang et al., 2017a,b). The DOPA-containing mussel mimicking proteins having sizable proportion of anionic phosphoserine residues have been utilized to form complex coacervates with the corresponding proteins containing cationic 4-hydroxyarginine residues. The phase-separated coacervates is an essential feature for wet adhesion (Lee et al., 2007; Shao and Stewart, 2010; Zhao et al., 2005). Catechol-based monomers, like *N*-(3,4-dihydroxyphenethyl) methacrylamide (Zhang et al., 2012), and 3,4-dihydroxystyrene (Pan et al., 2010) have been polymerized to obtain mussel mimetic adhesive polymers (Lee et al., 2004, 2007). The mussel-inspired chemistry has led to the surface modification of membranes by depositing catecholamines to improve their performance (Yang et al., 2015). Cross-linking of graphene oxide- or carbon nanotube-decorated polydopamine by polyethyleneimine (Guo et al., 2020) has broaden the utilization of graphene (Tian et al., 2013). Novel polymeric fluorescent organic nanoparticles have been fabricated via self-polymerization of dopamine and polyethyleneimine and further functionalized with other functional components for potential biological imaging applications (Shi, et al., 2017; Liu, et al., 2015). Several review articles discussed the mussel-inspired polydopamine (PDA)-based functional materials for environmental, energy, catalytical, and biomedical applications (Huang et al., 2020; Huang et al., 2018; Zhang et al., 2017a,b; Liu et al., 2016). MoS_2-PolyDOPA and other related composites have been shown to exhibit much enhanced adsorption capability towards methylene blue (Huang et al., 2017) and toxic metal ions (Gan et al., 2020; Dou et al., 2020), while MoS_2-PDA-Ag nanocomposites have been utilized as heterogeneous catalysts and antimicrobial agents (Zeng et al., 2018).

The ring-opening polymerization of epoxides using a variety of catalysts has been detailed in several review articles, which describe the synthesis of homo- and block copolymers (Brocas et al., 2013; Herzberger et al., 2016; Sarazin and Carpentier, 2015). It is our objective to use sesamol **1** as part of an epoxide **3** which could be used to obtain ring-opened mussel-inspired homo and copolymers (Scheme 1). Sesamol is chosen for two reasons: (i) it is a readily available natural product and (ii) to explore new avenue to put electron-rich triphenoxy motifs in a polymer chain. Sesamol **1** is a component of sesame seeds and sesame oil. Sesamol has been found to be an antioxidant (Kim et al., 2003; Toshiko, 1991), and can act as an antifungal (Wynn et al., 1997). Sesamol is used as a precursor in the industrial synthesis of the pharmaceutical drug paroxetine (Paxil) (Li et al., 2004). Sesame oil is used in Ayurvedic Medicine (Lahorkar et al., 2009). Chelation therapy is administered for the management of heavy metal-induced toxicity; a review article deals with the possible use and beneficial effects of sesame oil and sesamol during heavy metal toxicity treatment (Chandrasekaran et al., 2014). The natural edible sesame oil and the antioxidant sesamol are potently beneficial for treating lead- and iron-induced hepatic and renal toxicity and have no adverse effects (Chandrasekaran et al., 2014).

From synthetic perspective, the current study is intended to explore the chemistry of polymer chains embedded with highly electron-rich 1,3,4-triphenoxy motifs. Herein we report the ring-opening homopolymerization (Schemes 1 and 2) of sesamol-glycidyl ether **3** and its copolymerization (Scheme 3) with allyl glycidyl ether (AGE) **5**. The allyl pendants in the copolymer then could be elaborated to mussel-mimicking ionic polymers. The polymers may find application in the fields of adhesion, metal chelation, etc. The work would represent for the first time the ring-opening reaction of epoxide built upon the electron-rich motifs of hydroxyhydroquinone.

2. Experimental

2.1. Materials

tert-Butylammonium hydroxide (TBAH), $^{i}Bu_3Al$ solution (25 wt% in Toluene, 1 M), 2-butanone, allyl alcohol, 2,2-dimethoxy-2-phenylacetophenone (DMPA), cysteamine-HCl, thioglycolic acid and AGE were purchased from Aldrich Chemical. $MePPh_3Br$ from Fluka, 1 M tetrabutylammonium fluoride (TBAF) in THF from ChemCruz, were used as received. After drying over CaH_2, AGE was distilled. All solvents were of HPLC grade. Lead tetra acetate $Pb(AcO)_4$ was freshly prepared as described (Bailar et al., 1939). Membrane

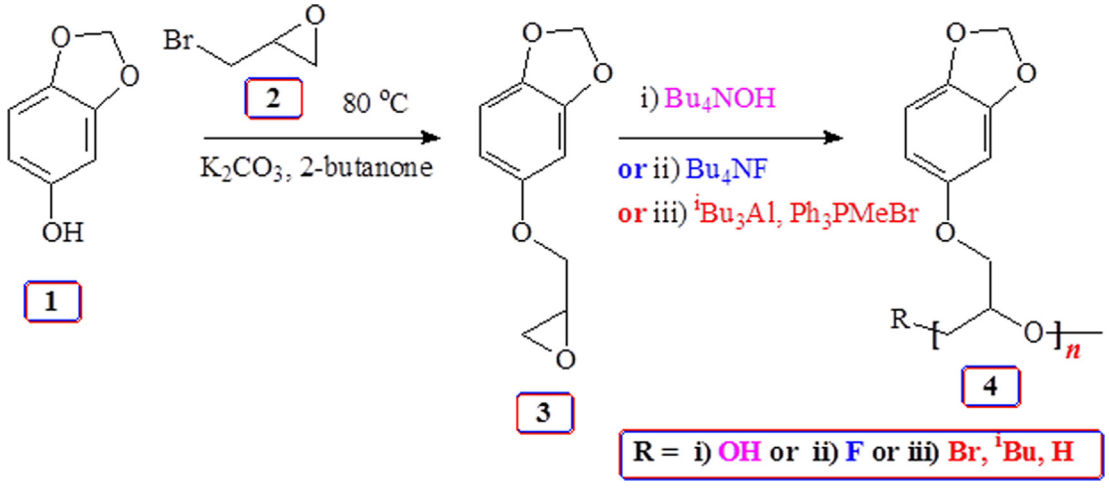

Scheme 1 Base as well as Lewis acid catalysed polymerization of sesamol-based epoxide **3**.

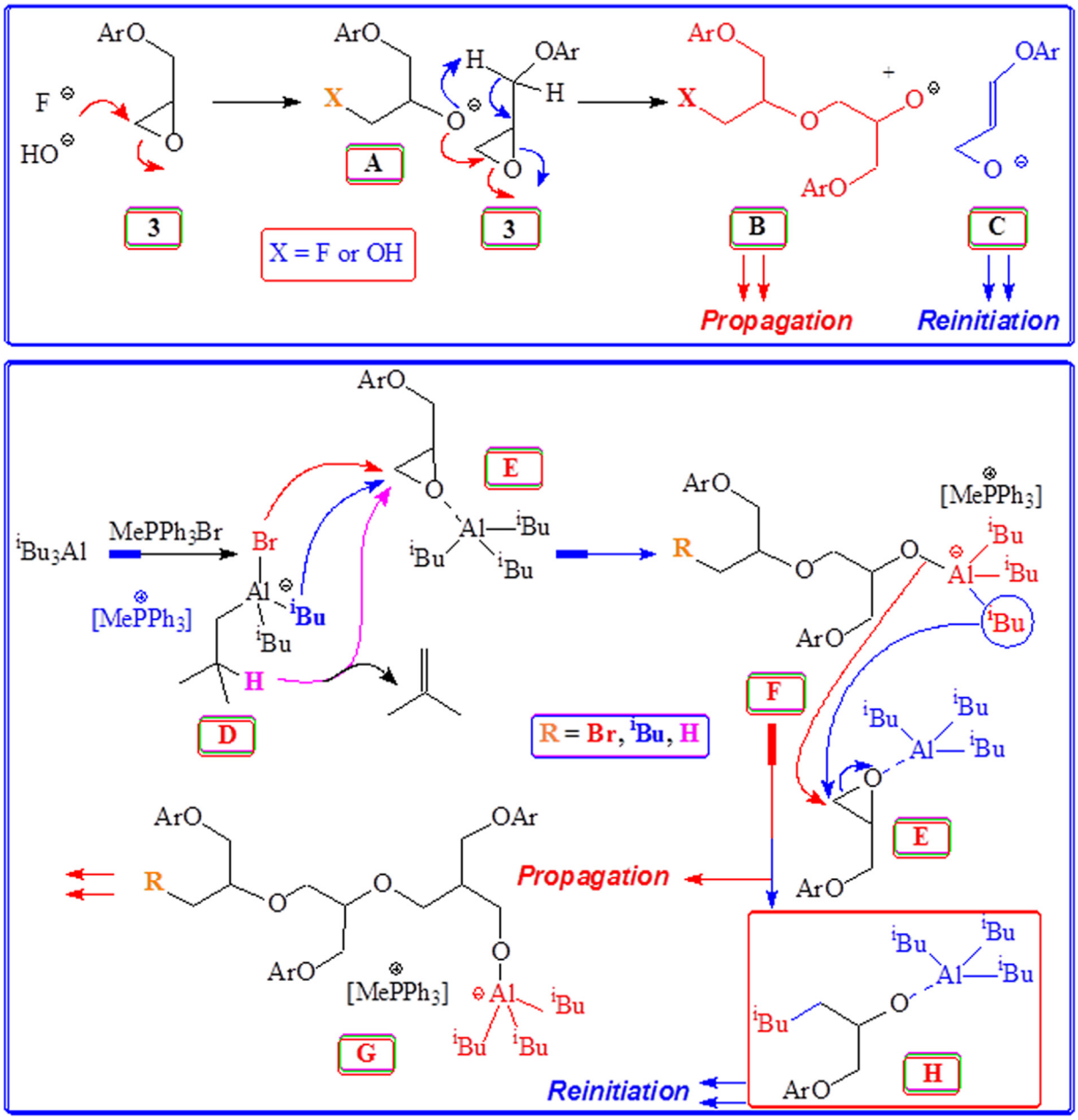

Scheme 2 Mechanism of base and acid catalyzed polymerization of monomer **3** using Bu_4NF, Bu_4NOH and $MePh_3PBr/^{i}Bu_3Al$.

(Spectra/Por, Spectrum Laboratories, Inc) with a MWCO of 6000–8000, was used for dialysis.

2.2. Physical methods

Atomic compositions were analysed in a Perkin Elmer (Series II Model 2400), while IR spectra were recorded on an FTIR spectrometer (Perkin Elmer 16F PC). NMR spectra were recorded in $CDCl_3$ with internal standard of tetramethylsilane (TMS) using a 500-MHz JEOL LA spectrometer. The TGA was carried out under O_2 by using an SDT analyser (Q600: TA Instruments). Epibromohydrin **2** was synthesised as described (Braun, 2003; Brunetto et al., 2002; Nelson et al., 1984). 3,4-methylenedioxy-1-oxyranylmethoxybenzene **3** was prepared in 77% yield by reacting sesamol **1** with epibromohydrin **2** as reported (Brizzi et al., 1999; Elzein et al., 2004; Wagner et al., 2004). GPC analysis was carried at 30 °C using a PL-GPC 220 containing two columns (PL aquagel-OH 8 μm; 300 × 7.5 mm) with Refractive Index & Light Scattering detectors (Agilent Technologies). [2,6-ditert-Butyl-4-methylphenol (BHT)] (0.0125 wt%), an antioxidant, was added to polymer solution in THF (5 mg/1.5 mL). Polystyrene standards were used to calibrate the instrument. A 100 μl polymer solution was used for chromatographic data analyzed using software by Agilent.

2.3. Polymerization of **3** using tetrabutylammonium derivatives (Eromosele and Pepper, 1989; Morinaga et al., 2011b, 2011a, 2007)

2.3.1. General procedure

Polymerization was carried out under conditions as described in Table 1 (entries 1–6). TBAF (1 M in THF) was placed in a

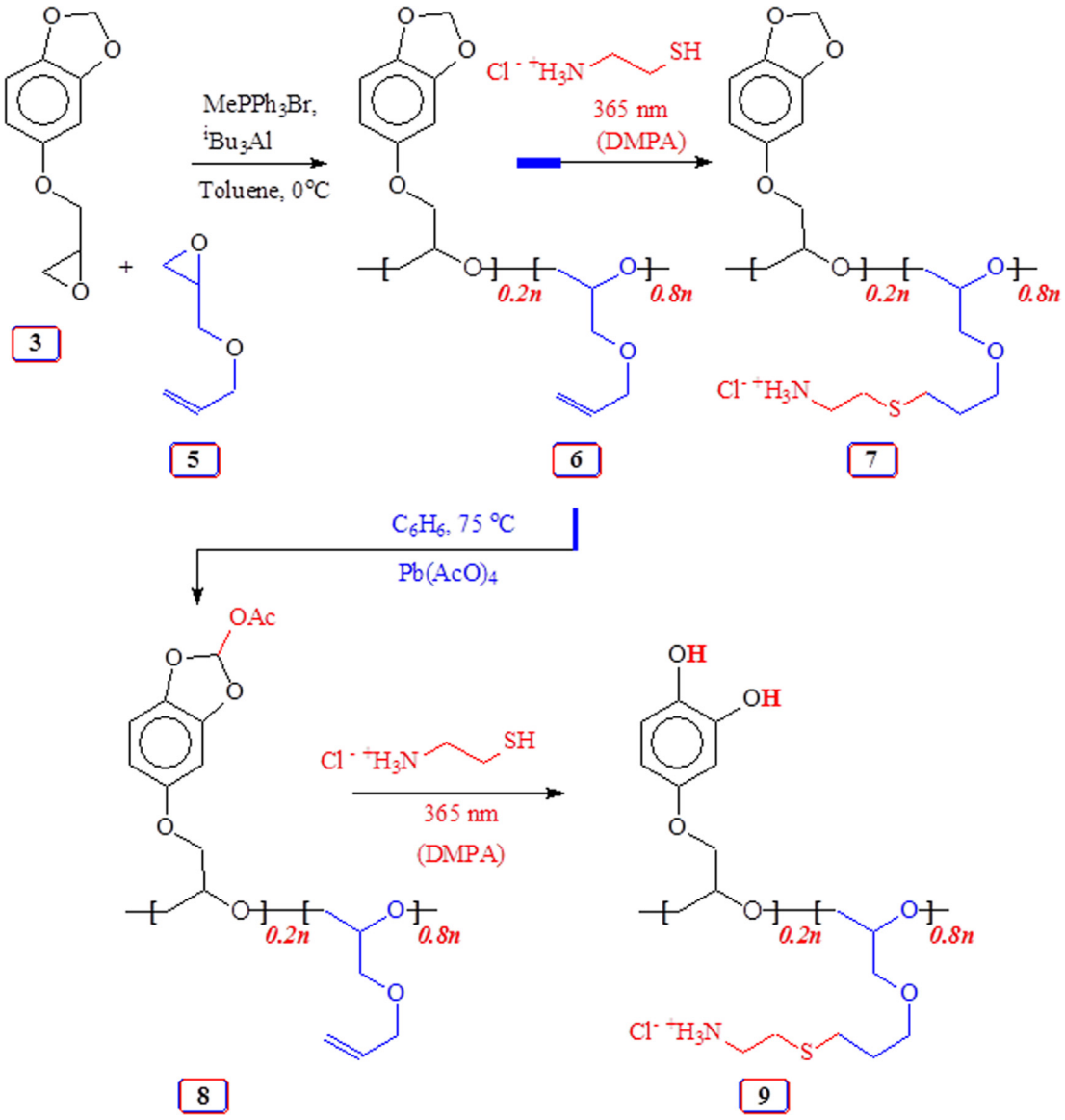

Scheme 3 Lewis acid catalyzed copolymerization of monomer **3**/allyl glycidyl ether **5** and thiol-ene and lead tetraacetate reaction of the copolymer.

flask, and the THF was removed under N_2. Monomer **3** was added and stirred at 50 °C until the reaction was complete as indicated by ^{1}H NMR spectrum. The reaction mixture was dissolved in CH_2Cl_2 and washed with water three times. After drying with Na_2SO_4, the organic layer was concentrated to obtain polymer **4**.

2.4. Time versus percent conversion of monomer *3* to polymer *4*

A specific reaction involved the use of TBAF (0.125 mmol from 1 M in THF). The TBAF in THF was taken in a flask and the solvent was removed under N_2 followed by vacuum. Monomer **3** (2.5 mmol) was then added and stirred at 50 °C. ^{1}H NMR spectra were recorded at several intervals and the results are given in Fig. 1. The percent conversion was determined using area integration of non-overlapping proton signals of polymer **4** and unreacted monomer **3** (Schemes 1 and 2).

2.5. Polymerization of *3* using $MePPh_3Br$ and $^iBu_3Al$

The conditions of the polymerization are given in Table 1 (entry 7). Monomer **3** (550 mg, 2.83 mmol) and 1.5 mL of dry toluene were injected under Ar through a rubber septum into an RB flask containing $MePPh_3Br$ (12.0 mg, 0.033 mmol). Then 1 M $^iBu_3Al$ in toluene (0.4 mL, 0.4 mmol) was injected under Ar as one portion to the reaction flask at 0 °C. After quenching the polymerization (2 h) with 80 v% MeOH/H_2O mixture (5 mL), the crude mixture was extracted with CH_2Cl_2, dried over anhydrous (Na_2SO_4), filtered over celite 545.and evaporated to obtain **4** as a solid (530 mg, 96%). (Found: C 61.6; H 5.1%. $C_{10}H_{10}O_4$ requires C 61.85; H 5.19%); $\nu_{max.}$

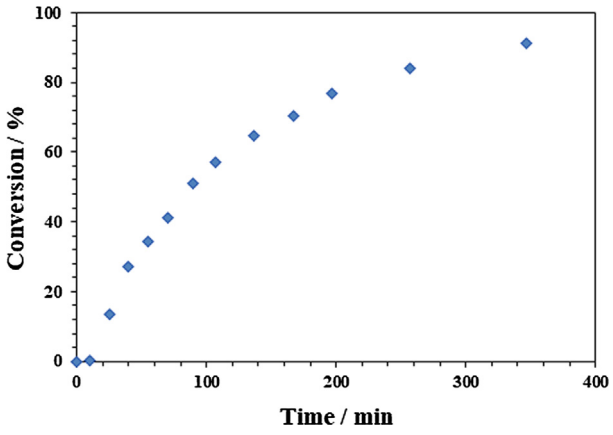

Fig. 1 Percent conversion of monomer **3** to polymer **4** under TBAF catalyzed polymerization.

KBr: 3527, 3086, 2879, 2778, 1633, 1510, 1287, 986, 922, 787, 738, 703, and 610 cm^{-1}.

*2.6. Random copolymerization of **3** and **5** by using $MePPh_3Br$ and $^iBu_3Al$*

The conditions for the polymerization are described in entry 8 (Table 1). Thus, monomer **3** (1.7 g, 8.6 mmol), AGE **5** (3.9 g, 33.8 mmol) were injected under Ar into an RB flask containing $MePPh_3Br$ (100 mg, 0.28 mmol). Then 1 M $^iBu_3Al$ in toluene (4.2 mL, 4.2 mmol) was injected under Ar as one portion to the reaction flask at 0 °C. When the ^1H NMR spectrum of the reaction mixture revealed the complete consumption of the monomers (≈6 h), the reaction was quenched by adding 80 v % $MeOH/H_2O$ mixture (50 mL). The solvents were removed from the mixture and the residue in CH_2Cl_2 (50 mL) was filtered over celite 545. Drying ($MgSO_4$) and removal of the solvent afforded random copolymer **6** (5.36 g, 96%) having a 20:80 ratio of the incorporated monomers **3** and **5** (Scheme 2). (Found: C 62.2; H 7.5%. Units of **3** and **5** in 20:80 requires C 62.75; H 7.74%); $\nu_{max.}$ KBr: 3485, 3081, 3017, 2919, 2866, 1635, 1496, 1355, 1255, 1192, 1134, 991, 925, 846, 738, 697, 614, and 561 cm^{-1}.

*2.7. Thiol–ene reaction (Campos et al., 2008; Ly et al., 2017) of cysteamine and vinyl bonds in **6***

A mixture of cysteamine. HCl (2.0 g, 19 mmol), photoinitiator DMPA (0.488 g, 1.9 mmol), were added to a solution of copolymer **6** (625 mg, containing 0.96 mmol of repeating units of **3** and 3.84 mmol repeating units **5**) in 2:1 THF/MeOH (4.5 mL) was irradiated under N_2 with a 365 nm UV lamp for 5 h. ^1H NMR spectrum revealed the complete disappearance of the alkene motifs of copolymer **6**. After washing with ether and dialysis of the residue against distilled water and freeze-drying afforded polymer **7** (0.86 g, 81%). (Found: C 44.7; H 7.6%. Repeat units **3** and cysteamine. HCl-incorporated **5** in 20:80 requires C 45.65; H 7.48%); $\nu_{max.}$ KBr: 3585, 3414, 3083, 2963, 1490, 1406, 1260, 1189, 1099, 1017, 869, 798, and 677 cm^{-1}.

Table 1 Homo- and copolymerization[a] of sesamol derived monomer (SD) **3** using various initiators (I) and its copolymerization with allyl glycidyl ether (AGE) **5**.

Entry	**I** (mmol)	[**SD**]/[**I**]	Time (h)	Conv.[b] (%)	$M_{n,Theor}$[c]	$M_{n,Exp}$[d]	PDI
Homopolymerization of monomer 3							
1	TBAF (0.10)	25	6	85			
			26	96	4,660	1532	1.2
2	TBAF (0.025)	100	6	1			
			24	7			
			32	11			
			69	89			
			93	93			
			117	95			
			141	98	19,030	1230	2.6
3	TBAF (0.075)	33	6	80			
			24	94			
			46	98	6,280	1529	1.2
4	TBAF (0.175)	14	18	99	2,690	1264	1.2
5	TBAF (0.225)	11	6	98	2,090	1169	1.3
6	TBAH (0.10)	25	6	98	4,760	2985	1.4
7	$MePPh_3Br$ (0.033)	86	2	96	16,030	8,750	1.6
Copolymerization of monomers 3 and 5							
8	$MePPh_3Br$ (0.28)	151[e]	6	96	18,920	9,570	1.7

[a] Homopolymerization of **3** (2.5 mmol) was carried out at 50 °C (entries 1–6), at 0 °C using **3** (2.83 mmol) catalysed by $^iBu_3Al$ (**C**) (0.4 mmol) (entry 7) and monomer **3** (8.6 mmol), **7** (33.8 mmol) catalysed by $^iBu_3Al$ (**C**) (4.2 mmol) (entry 8).

[b] Conversion as determined by ^1H NMR. Isolated yield of all the polymers were > 90% in most cases.

[c] M_n for entry 2 = [molar mass of SD] × [**SD**]/[**I**] × % conversion/100 = 194.19 × 100 × 0.98* = 19,030. M_n for entry 8 = [molar mass of SD × 0.20 + molar mass of allyl glycidyl ether (AGE) × 0.80] × [**SD** + **AGE**]/[**I**] × % conversion/100 = [194.19 × 0.20 + 114.14 × 0.80] × [(8.6 + 33.8)/0.28] × 0.96 = 18,920.

[d] GPC with a light scattering detector.

[e] [**SD 3** + **AGE 5**]/[**I**].

2.8. Lead tetraacetate oxidation (Lee et al., 2009; Nicolaou et al., 2010) to activate O-CH_2-O in copolymer ***6***

A solution of copolymer **6** (Entry 8, Table 1) (1.90 g, containing 2.92 mmol of repeating units of **3** and 11.68 mmol of units of **5**) in benzene (25 mL) was reacted with $Pb(OAc)_4$ (2.0 g, 4.5 mmol) under stirring condition at 75 °C under N_2 for 24 h. After washing the crude mixture in EtOAc (35 mL) with H_2O (3 × 30 mL), and removal of the organic solvents gave **8** (1.66 g, 80%). (Found: C 60.3; H 7.5%. Units of **3**-OAc and **5** in 20:80 requires C 61.00; H 7.39%); $\nu_{max.}$ KBr: 3503, 3080, 3015, 2927, 2869, 1759, 1645, 1613, 1497, 1367, 1224, 1189, 917, 844, 789, 758, 711, 669, 615, and 560 cm^{-1}.

2.9. Thiol–Ene reaction (Campos et al., 2008) of cysteamine to vinyl double bonds in ***8***

To a solution of copolymer **8** (0.30 g, containing 0.42 mmol of repeating units of **3-OAc** and 1.69 mmol of units of **5**) in

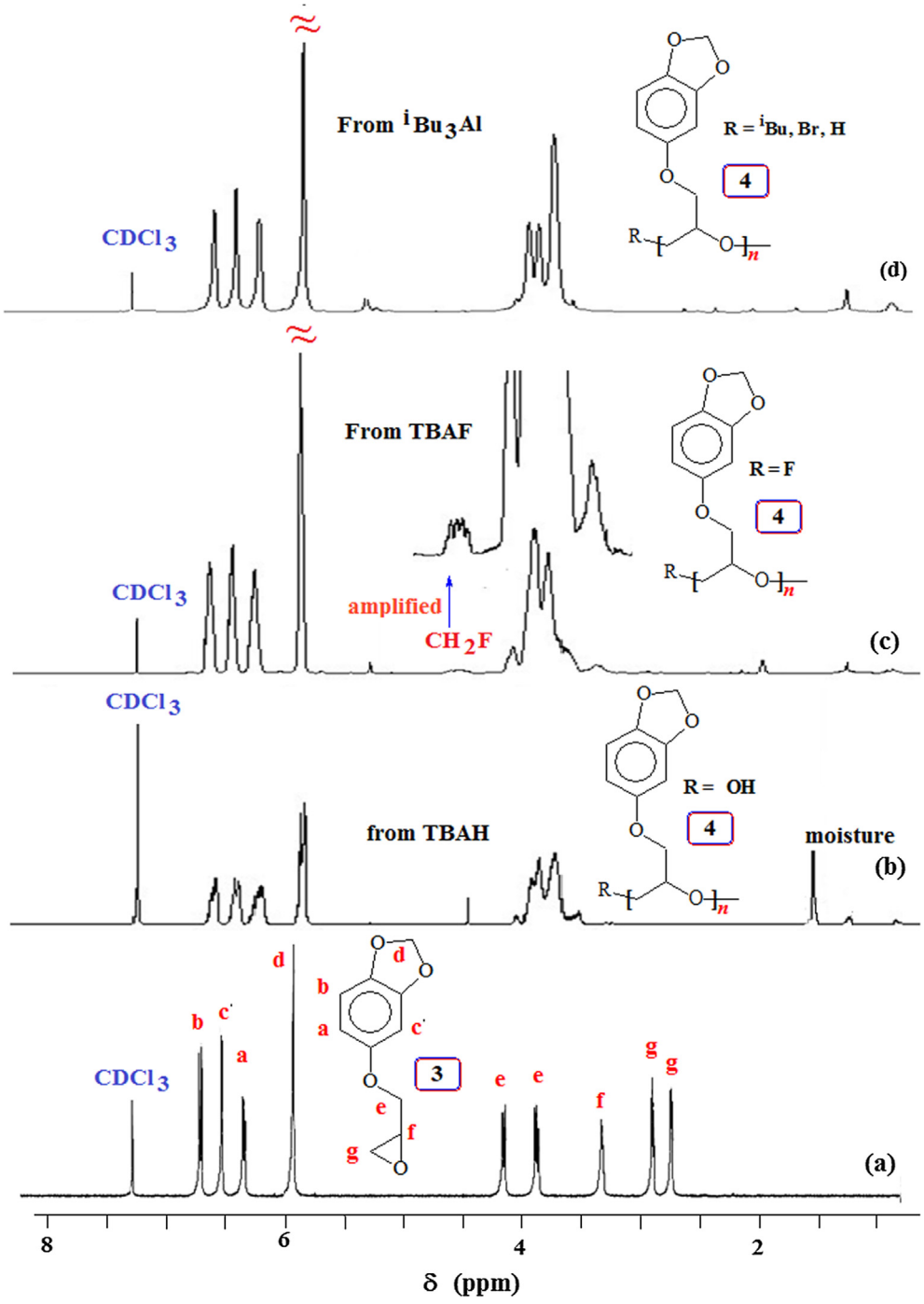

Fig. 2 ^{1}H NMR spectra in $CDCl_3$ of (**a**) monomer **3**; and polymer **4** obtained using initiator (**b**) Bu_4NOH (TBAH), (**c**) Bu_4NF (TBAF) and (**d**) $^{i}Bu_3Al/MePh_3PBr$.

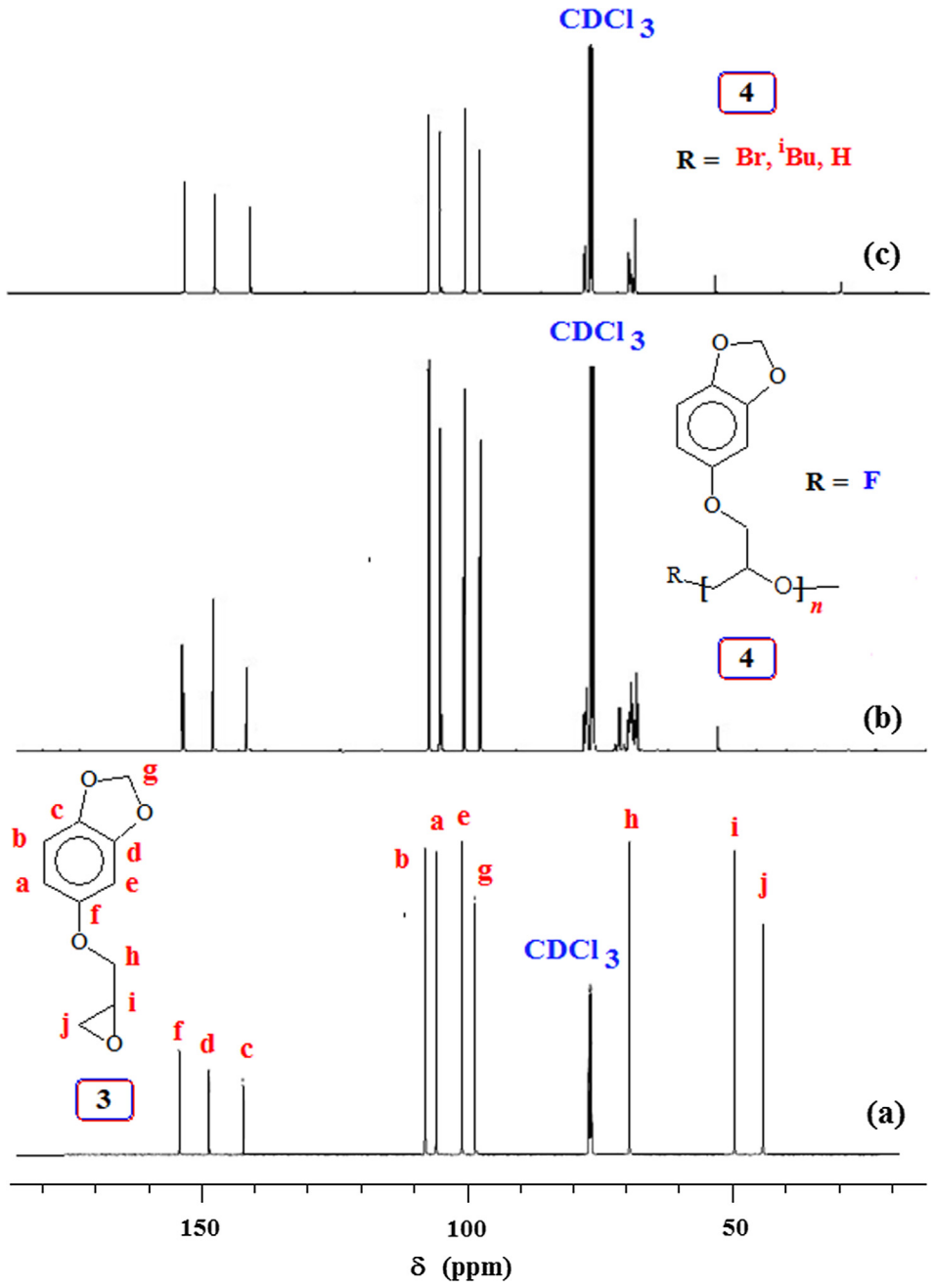

Fig. 3 ^{13}C NMR spectra in $CDCl_3$ of (**a**) monomer **3**; and polymer **4** obtained using initiator (**b**) Bu_4NOH (TBAH), (**c**) Bu_4NF (TBAF) and (**d**) $^{i}Bu_3Al/MePh_3PBr$.

2:1 THF/MeOH (3.5 mL) was added cysteamine.HCl (0.96 g, 8.4 mmol) and photoinitiator DMPA (0.215 g, 0.84 mmol). The mixture after purging with N_2 was irradiated with a 365 nm UV lamp for 6 h for complete reaction of the double bonds in the polymer **8** as indicated by a ^{1}H NMR spectrum. The photoinitiator from the crude mixture was removed by washing it with ether. The mixture upon dialysis (against 0.1 M HCl followed by against distilled water), and freeze-drying afforded polymer **9** (0.36 g, 78%) as a solid. $\nu_{max.}$ KBr: 3471, 3424, 3081, 2917, 2869, 1622, 1488, 1354, 1257, 1189, 1101, 1029, 928, 801, 678, and 554 cm^{-1}.

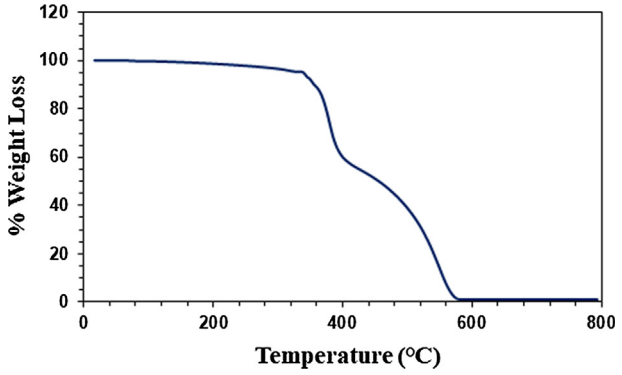

Fig. 4 TGA curve of polymer 4.

*2.10. Thiol–Ene reaction (Campos et al., 2008) of thioglycolic acid to vinyl double bonds in **6***

A mixture of thioglycolic acid (1.75 g, 19 mmol), DMPA (488 mg, 1.9 mmol), copolymer **6** (Entry 8, Table 1) (625 mg, containing 0.96 mmol of repeating units of **3** and 3.84 mmol of units **5**) in THF (3 mL) was irradiated under N_2 as before (6 h). The crude product was repeatedly washed with ether to remove the photoinitiator, thereafter transferred to a dialysis bag with the help of methanol/THF and dialyzed

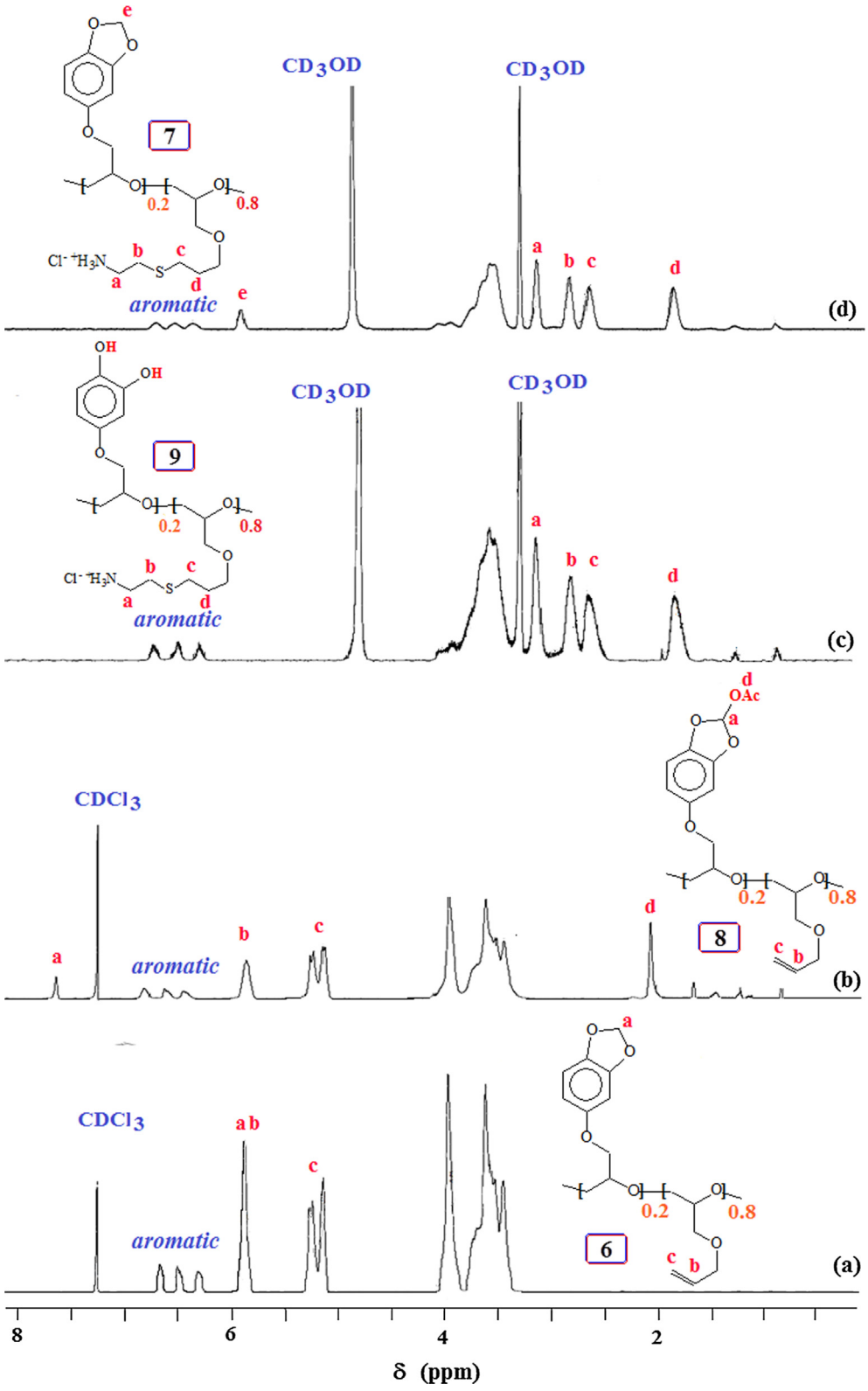

Fig. 5 ^{1}H NMR spectra in $CDCl_3$ of copolymer (**a**) **6**, and (**b**) **8**; and in CD_3OD of copolymer (**c**) **9** and (**d**) **7**.

against distilled water (24 h). After freeze-drying, the polymer was obtained as a thick colorless liquid of **10** (805 mg, 82%). The polymer was insoluble in water or methanol or $CHCl_3$. However, the polymer was readily soluble in 20:1 $CHCl_3$/MeOH mixture. ν_{max}. (neat): 3500 (br), 2924, 2876, 1724, 1632, 1487, 1273, 1188, 1120, 1038, 923, 817, 788, 649 and 577 cm^{-1}. (Found: C 49.0; H 6.7; S, 11.8%. Units of **3** and **5** (after thiol-ene reaction) in 20:80 requires C, 49.50; H, 6.53; S, 12.58%).

3. Results and discussion

Epibromohydrin **2** was prepared as described in Scheme 1. Sesamol **1** was alkylated using **2** to obtain epoxide monomer **3**. The polymerization reaction was carried out using base or Lewis acid catalysed ring-opening process to obtain polyether **4** having the pendants of sesamol residues. Polymerization catalysed by Bu_4NOH is expected have 'OH' groups on both terminals, while catalysis by Bu_4NF (TBAF) is expected to insert 'F' on one end of the chain.

Conversion versus time profile for the polymerization reaction cried out under TBAF catalysis is shown in Fig. 1. The percent conversion after a time interval was determined by ^{1}H NMR technique; at each interval, a small portion of the reaction mixture was withdrawn and quenched to terminate the propagation process. Fig. 1 reveals that 50% conversion had occurred after 90 min.

The results of the polymerizations are given in (Table 1). The Table includes polydispersity index (PDI) and molar masses. The $\bar{M}_n$ values were determined to be less than the theoretical values thereby suggesting chain transfer rection. The polymerization reactions afforded polymer in excellent yield (Table 1). The polymerization catalyzed by TBOH (entry 6, Table 1) gave polymer with a higher molar mass than that of the polymer obtained via TBAF-initiation (entries 1–5).

The F^- or OH^- or the propagating alkoxide ion '**A**' (RO^-) may involve in nucleophilic ring-opening (red arrows) propagation to '**B**' as well as base catalysed proton abstraction (blue arrows) to '**C**' as depicted in Scheme 2. The chain transfer to monomer **3** and subsequent re-initiation by species '**C**' could lower the molar mass of the polymers as confirmed by the GPC results whereby the observed molar masses are much less as compared to theoretically expected values (entries 1–6, Table 1). Note that: in alkali metal alkoxides catalysed polymerization of propylene oxide (PO) [$CH_3(CHCH_2)O$], the highly basic macroanion RO^- is known to abstract H from CH_3 group of the monomer causing a chain transfer to the monomer (Boileau, 1989; Gagnon, 1985; Quirk and Lizarraga, 2000).

The above findings have prompted us to carry out the polymerization under Lewis acid catalysis which may minimize the chain transfer process (*vide supra*). The polymerization of **3** using Lewis acid catalyst ^{i}Bu_3Al and initiator (**I**) $MePh_3PBr$ (Alhaffar et al., 2019; Billouard et al., 2004; Sakakibara et al., 2007, 2006) gave polyether **4** in excellent yield (entry 7, Table 1) (Scheme 1). For the successful polymerization [^{i}**Bu$_3$Al**]/[**I**] is kept $\geq$1, since the aluminate complex as depicted by '**D**' (Scheme 2) is not enough a reactive nucleophile to initiate the polymerization. The process also requires the activation of monomer **3** in the presence of an excess of ^{i}Bu_3Al thereby ensuring active participation of the enhanced electrophilic complex species '**E**'. The experimental molar mass of polymer **4** as obtained by GPC is less than the theoretical value based on each $Ph_3MeP^+Br^-$ forming one polymer chain (see Table 1). Thus, the polymerization of monomer **3** encounters chain transfer process involving complex '**F**' whereby normal propagation as depicted by the red arrow leads to '**G**', while the transfer of ^{i}Bu group to monomer complex '**E**' as indicated by the blue arrow gives '**H**' which can re-initiate a new polymer chain (Scheme 2). The initiation process as depicted in species '**D**' is known to involve nucleophilic attack by Br^- as well as by $^iBu^-$ and hydride anion (Sakakibara et al., 2007, 2006) thereby leading to three types of end groups (Boireau et al., 1980; Eisch et al., 1992).

The ^{1}H and ^{13}C NMR spectra of monomer **3** and its corresponding polymers using different initiators are shown in Figs. 2 and 3, respectively. There are minor differences in the ^{1}H spectrum of **4** obtained by base and Lewis acid catalyzed polymerization (cf. Fig. 2b,c vs. d) in the region of δ3.5 ppm. Note that the CH_2F protons attached at one end of **4** is displayed at δ4.6 ppm as a minor signal (Fig. 2c)

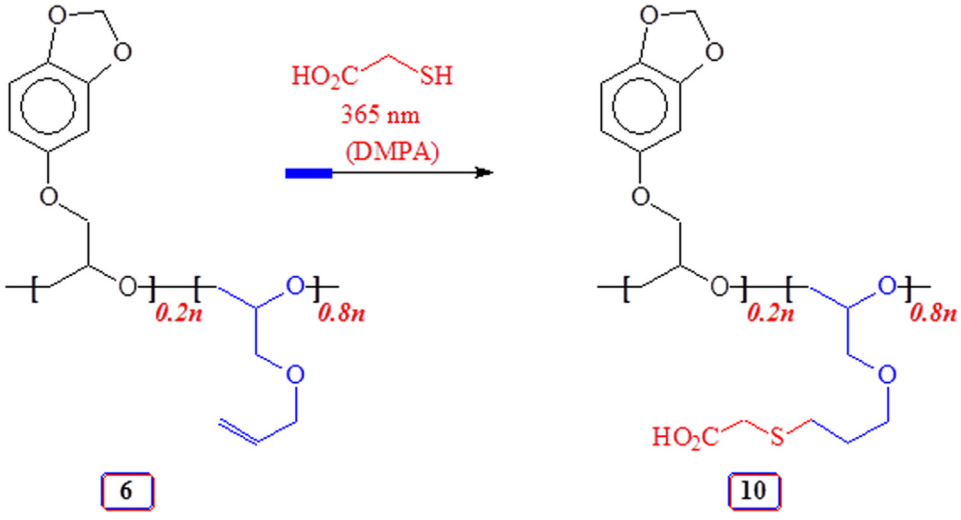

Scheme 4 Thiol-ene reaction of copolymer **6** with thioglycolic acid.

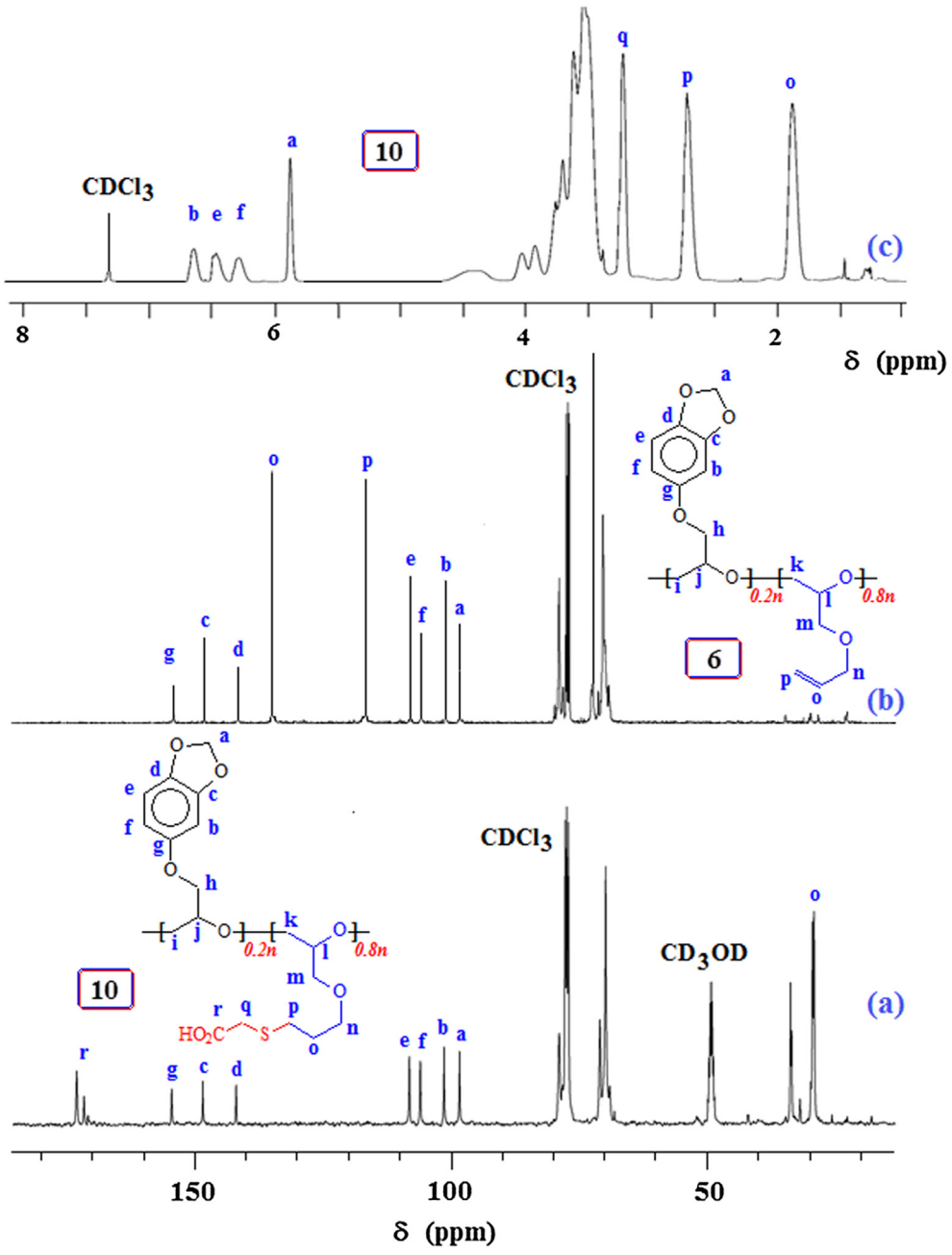

Fig. 6 ^{13}C NMR spectra of (**a**) **10** in 20:1 $CDCl_3/CD_3OD$, and (**b**) **6** in $CDCl_3$; and (**c**) ^{1}H NMR spectrum of **10** in 20:1 $CDCl_3/CD_3OD$.

(Morinaga et al., 2011b, 2007). End group analysis involving area integration of CH_2F protons versus the aromatic proton signals (Fig. 2c) and assuming a CH_2F group per polymer chain h, the TBAF-initiated polymer sample **4** from entry 4 (Table 1) revealed its molar mass ($\bar{M}_n$) as 4850 g mol^{-1}. The experimental $\bar{M}_n$ value of 1264 (Table 1) therefore suggests the involvement of extensive chain transfer and as such considerable of number of polymer chains do not have CH_2F terminal. While the signal pattern of the aromatic carbons remains similar in the monomer and polymer, there are some differences in the complexity of the carbons attached to oxygen as a result of differences in the microstructure of the polymers obtained via base or Lewis acid catalyzed polymerization (Fig. 3).

The thermogravimetric analysis (TGA) curve of polymer **4** is shown in Fig. 4. The first weight loss 9% up to 350 °C is accounted for the removal of trapped solvent and moisture. The second loss of about 34% in the range 350–413 °C could be attributed to the removal of CH_2CHCH_2O motifs, calculated to constitute 30%, from the polymer backbone. Polyethylene glycols are known to decompose in that range (Kwon and Kim, 2006). The third loss of 56% in the range 423–594 °C is accounted by the loss of aromatic motifs containing three oxygens. At 793 °C, the residual mass was found to be 0.9%. The polymer is thus found to be very stable up to 350 °C.

Copolymerization of **3** and **5** under Lewis acid catalysis afforded copolymer **6** in 96% yield (entry 8, Table 1); the

polymer upon thiol-ene reaction (Campos et al., 2008) using cysteamine.HCl gave **7** (Scheme 3). To mimic mussel-inspired polymers, methylene acetal, a robust protective group that could not be deprotected under acid, in the current polymers must be deprotected to diol motifs. To circumvent the problem, the O-CH_2-O motifs in **6** were activated using lead tetraacetate (Lee et al., 2009; Nicolaou et al., 2010) to obtain **8** containing the labile acetoxy substituent. Polyether **8** was then elaborated by thiol-ene reaction which converted it to **9**; during dialysis in the presence of 0.1 M HCl, the facile deprotection took place.

The ^{1}H NMR spectra of **6**–**9** are shown in Fig. 5. Copolymer **6** with a 20:80 ratio of repeating unit of sesamol-derived monomer **3** and AGE **5** was used for its conversion to **7**–**9**. The ratio of the incorporated monomers was determined by area integration of several signals such as three aromatic Hs versus two alkene Hs marked 'c' (Fig. 5a). The presence of acetyl proton marked 'd' in —CHOCOC$\underline{H}_3$ and acetal proton —C$\underline{H}$OCOCH_3 marked 'a' in Fig. 5(b), confirms the formation of **8** having a labile protection group. Alkenes protons disappeared after thiol-ene reaction in the spectra of **9** (Fig. 5c) and **7** (Fig. 5d). The NMR spectra confirmed the incorporation cysteamine motifs.

Towards the end, copolymer **6** was elaborated via thiol-ene reaction with thioglycolic acid to **10** having anioinic-CO_2^- groups (Scheme 4). Fig. 6 displays the NMR spectra of **6** and **10**. The alkene C marked '**o**' and '**p**' in copolymer **6** (Fig. 6b) disappeared upon thiol-ene reaction as can be seen from the of ^{13}C spectrum of **10** in Fig. 6(a); the corresponding ^{1}H spectrum in Fig. 6(c) also reveals the absence of alkene protons at $\approx \delta$ 5.5 ppm.

4. Conclusions

Monomer **3** has been prepared in very good yield (77%) by reacting naturally occurring sesamol **1** with epibromohydrin **2**. To our knowledge, oxide **3** derived from naturally occurring sesamol**,** has been homo- as well as copolymerized with AGE **5** for the first time. Monomer **3** underwent ring-opening polymerization using basic Bu_4NOH and Bu_4NF as well as by Lewis acid initiator/catalyst to polyether **4** in 80–99% yields. The random copolymer **6** was obtained *via* ring-opening copolymerization of **3/5** pair using Lewis acid initiator/catalyst in 96% yield. Copolymer **6** was elaborated by incorporating cationic (NH_3^+) and anionic (CO_2^-) groups on the pendants *via* photo-initiated thiol-ene reaction of copolymer **6** with cysteamine.HCl and thioglycolic acid to give **7** (81% yield) and **10** (82% yield), respectively. The activation of the O-CH_2-O motifs in **6** using lead tetraacetate gave **8** containing the labile acetoxy substituent in 80% yield. Polymer **8** upon thiol-ene reaction with cysteamine.HCl followed by aqueous work up afforded **9** (90% yield) having deprotected catechol units in the macromolecule. The synthesised polymers have an exciting feature of electron-rich hydroxyhydroquinone motifs which mimics mussel-inspired polymers containing catechol units. Catechol motifs are known for their efficacy in adsorption of metal ions from aqueous solution (Li et al., 2010). Currently we are investigating the adsorption of metal ions in aqueous solution by theses polymers as well as their performance for inhibition of the mild steel corrosion.

Declaration of Competing Interest

The authors declared that there is no conflict of interest.

Acknowledgments

The authors would like to acknowledge the support provided by King Abdulaziz City for Science and Technology (KACST), Saudi Arabia through the Science & Technology Unit at King Fahd University of Petroleum & Minerals (KFUPM), Saudi Arabia for funding this work through project No. 12-ADV2397-04 as part of the National Science, Technology and Innovation Plan.

References

Ahmadi, Z., 2019. Nanostructured epoxy adhesives: A review. Prog. Org. Coat. 135, 449–453. https://doi.org/10.1016/j.porgcoat.2019.06.028.

Alhaffar, M.T., Akhtar, M.N., Ali, S.A., 2019. Utilization of catecholic functionality in natural safrole and eugenol to synthesize mussel-inspired polymers. RSC Adv. 9, 21265–21277. https://doi.org/10.1039/C9RA04719K.

Bailar, J.C., Fernelius, W.C., Skinner, H.A., 1939. Lead Tetiucetate. Inorg. Synth. 1, 47–49. https://doi.org/10.1002/9780470132326.ch17.

Basiri, Z., Rezayan, A.H., Akbari, B., Aghdam, R.M., Tafti, H.A., 2018. Developing new synthetic biomimetic nanocomposite adhesives: Synthesis and evaluation of bond strength and solubilization. React. Funct. Polym. 127, 85–93. https://doi.org/10.1016/j.reactfunctpolym.2018.04.004.

Billouard, C., Carlotti, S., Desbois, P., Deffieux, A., 2004. "Controlled" high-speed anionic polymerization of propylene oxide initiated by alkali metal alkoxide/trialkylaluminum systems. Macromolecules 37, 4038–4043. https://doi.org/10.1021/ma035768t.

Boileau, S., 1989. In comprehensive polymer science, chain polymerization. In: Vol. 3, Part 1. pp. 467–487.

Boireau, G., Abenhaim, D., Henry-Basch, E., 1980. The ate complexes of aluminium. Reactivity and stereoselectivity with respect to epoxides and carbonyl compounds. Catalytic activation by salts of transition metals. Tetrahedron 36, 3061–3070. https://doi.org/10.1016/0040-4020(80)88033-1.

Braun, G., 2003. Epichlorohydrin and Epibromohydrin. Org. Synth. 16, 30. https://doi.org/10.1002/0471264180.os016.10.

Brizzi, V., Francioli, M., Brufani, M., Filocamo, L., Bruni, G., Massarelli, P., 1999. Synthesis, binding affinity and selectivity of new β1- and β2-adrenoceptor blockers. Farmaco 54, 713–720. https://doi.org/10.1016/S0014-827X(99)00077-4.

Brocas, A.-L., Mantzaridis, C., Tunc, D., Carlotti, S., 2013. Polyether synthesis: From activated or metal-free anionic ring-opening polymerization of epoxides to functionalization. Prog. Polym. Sci. 38, 845–873. https://doi.org/10.1016/j.progpolymsci.2012.09.007.

Brunetto, G., Gori, S., Fiaschi, R., Napolitano, E., 2002. Crystallization-induced asymmetric transformations. Enantiomerically pure (-)-(R)- and (+)-(S)-2,3-dibromopropan-1-ol and epibromohydrins. A study of dynamic resolution via the formation of diastereoisomeric esters. Helv. Chim. Acta 85, 3785–3791. https://doi.org/10.1002/1522-2675(200211)85:11<3785::AID-HLCA3785>3.0.CO;2-A.

Campos, L.M., Killops, K.L., Sakai, R., Paulusse, J.M.J.J., Damiron, D., Drockenmuller, E., Messmore, B.W., Hawker, C.J., 2008. Development of thermal and photochemical strategies for thiol-ene click polymer functionalization. Macromolecules 41, 7063–7070. https://doi.org/10.1021/ma801630n.

Chandrasekaran, V.R.M., Hsu, D.-Z., Liu, M.-Y., 2014. Beneficial effect of sesame oil on heavy metal toxicity. J. Parenter. Enter. Nutr. 38, 179–185. https://doi.org/10.1177/0148607113490960.

Comyn, J., 1981. The relationship between joint durability and water diffusion. In: Kinloch, A.J., (Ed.), vol. 2. Barking, Appl. Sci. Publ., UK, pp. 279–313.

Dou, J., Chen, J., Huang, Q., Huang, H., Mao, L., Deng, F., Wen, Y., Zhu, X., Zhang, X., Wei, Y., 2020. Preparation of polymer functionalized layered double hydroxide through mussel-inspired chemistry and Kabachnik-Fields reaction for highly efficient adsorption. J. Environ. Chem. Eng. 8 (2020), 103634. https://doi.org/10.1016/j.jece.2019.103634.

Eisch, J.J., Liu, Z.R., Singh, M., 1992. Organometallic compounds of Group III. 48. High regioselectivity in the alternative, reductive cleavages of terminal epoxides with aluminum reagents. J. Org. Chem. 57, 1618–1621. https://doi.org/10.1021/jo00031a058.

Elzein, E., Shenk, K., Ibrahim, P., Marquart, T., Kerwar, S., Meyer, S., Ahmed, H., Zeng, D., Chu, N., Soohoo, D., Wong, S., Leung, K., Zablocki, J., 2004. Novel inhibitors of fatty acid oxidation as potential metabolic modulators. Bioorganic Med. Chem. Lett. 14, 973–977. https://doi.org/10.1016/j.bmcl.2003.11.065.

Eromosele, I.C., Pepper, D.C., 1989. Anionic polymerization of butyl cyanoacrylate by tetrabutylammonium salts, 2. Propagation rate constants. Die Makromol. Chemie 190, 3095–3103. https://doi.org/10.1002/macp.1989.021901207.

Gagnon, S.D., 1985. In Encyclopedia of polymer science and engineering. In: Quirk, R.P. (Ed.), vol. 6. Wiley-Interscience, New York, pp. 273–307.

Gan, D., Huang, Q., Dou, J., Huang, H., Chen, J., Liu, M., Wen, Y., Yang, Z., Zhang, X., Wei, Y., 2020. Bioinspired functionalization of MXenes ($Ti_3C_2T_X$) with amino acids for efficient removal of heavy metal ions. Appl. Surf. Sci. 504, 144603. https://doi.org/10.1016/j.apsusc.2019.144603.

Guo, L., Liu, Y., Dou, J., Huang, Q., Lei, Y., Chen, J., Wen, Y., Li, Y., Zhang, X., Wei, Y., 2020. Surface modification of carbon nanotubes with polyethyleneimine through "mussel inspired chemistry" and "Mannich reaction" for adsorptive removal of copper ions from aqueous solution. J. Environ. Chem. Engi. 8, 103721. https://doi.org/10.1016/j.jece.2020.103721.

Herzberger, J., Niederer, K., Pohlit, H., Seiwert, J., Worm, M., Wurm, F.R., Frey, H., 2016. Polymerization of ethylene oxide, propylene oxide, and other alkylene oxides: synthesis, novel polymer architectures, and bioconjugation. Chem. Rev. 116, 2170–2243. https://doi.org/10.1021/acs.chemrev.5b00441.

Huang, Q., Chen, J., Liu, M., Huang, H., Zhang, X., Wei, Y., 2020. Polydopamine-based functional materials and their applications in energy, environmental, and catalytic fields: State-of-the-art review. Chem. Eng. J. 387, 124019. https://doi.org/10.1016/j.cej.2020.124019.

Huang, L., Liu, M., Huang, H., Wen, Y., Wen, Y., 2018. Recent advances and progress on melanin-like materials and their biomedical applications. Biomacromolecules 19, 1858–1868. https://doi.org/10.1021/acs.biomac.8b00437.

Huang, Q., Liu, M., Chen, J., Wan, Q., Tian, J., Huang, L., Jiang, R., Wen, Y., Zhang, X., Wei, Y., 2017. Facile preparation of MoS_2 based polymer composites via mussel inspired chemistry and their high efficiency for removal of organic dyes. Appl. Surf. Sci. 419, 35–44. https://doi.org/10.1016/j.apsusc.2017.05.006.

Jouyandeh, M., Jazani, O.M., Navarchian, A.H., Shabanian, M., Vahabi, H., Saeb, M.R., 2019. Bushy-surface hybrid nanoparticles for developing epoxy superadhesives. Appl. Surf. Sci. 479, 1148–1160. https://doi.org/10.1016/j.apsusc.2019.01.283.

Jouyandeh, M., Jazani, O.M., Navarchian, A.H., Shabanian, M., Vahabi, H., Saeb, M.R., 2018a. Surface engineering of nanoparticles with macromolecules for epoxy curing: Development of super-reactive nitrogen-rich nanosilica through surface chemistry manipulation. Appl. Surf. Sci. 447, 152–164. https://doi.org/10.1016/j.apsusc.2018.03.197.

Jouyandeh, M., Paran, S.M.R., Shabanian, M., Ghiyasi, S., Vahabi, H., Badawi, M., Formela, K., Puglia, D., Saeb, M.R., 2018b. Curing behavior of epoxy/Fe_3O_4 nanocomposites: A comparison between the effects of bare Fe_3O_4, Fe_3O_4/SiO_2/chitosan and Fe_3O_4/SiO_2/chitosan/imide/phenylalanine-modified nanofillers. Prog. Org. Coat. 123, 10–19. https://doi.org/10.1016/j.porgcoat.2018.06.006.

Kaushik, N., Kaushik, N., Pardeshi, S., Sharma, J., Lee, S., Choi, E., ushik et al. 2015,. Biomedical and clinical importance of mussel-inspired polymers and materials. Mar. Drugs. https://doi.org/10.3390/md13116792.

Kim, J.Y., Choi, D.S., Jung, M.Y., 2003. Antiphoto-oxidative activity of sesamol in methylene blue- and chlorophyll-sensitized photo-oxidation of oil. J. Agric. Food Chem. 51, 3460–3465. https://doi.org/10.1021/jf026056p.

Kwon, S.K., Kim, D.H., 2006. Effect of process PARAMETERS of UV-assisted gas-phase cleaning on the removal of PEG (Polyethyleneglycol) from a Si substrate. J. Korean Phys. Soc. 49, 1421–1427 https://www.researchgate.net/publication/264542305.

Lahorkar, P., Ramitha, K., Bansal, V., Anantha Narayana, D., 2009. A comparative evaluation of medicated oils prepared using ayurvedic and modified processes. Indian J. Pharm. Sci. 71, 656. https://doi.org/10.4103/0250-474X.59548.

Lee, B.P., Huang, K., Nunalee, F.N., Shull, K.R., Messersmith, P.B., 2004. Synthesis of 3,4-dihydroxyphenylalanine (DOPA) containing monomers and their co-polymerization with PEG-diacrylate to form hydrogels. J. Biomater. Sci. Polym. Ed. 15, 449–464. https://doi.org/10.1163/156856204323005307.

Lee, B.P., Messersmith, P.B., Israelachvili, J.N., Waite, J.H., 2011. Mussel-inspired adhesives and coatings. Annu. Rev. Mater. Res. 41, 99–132. https://doi.org/10.1146/annurev-matsci-062910-100429.

Lee, H., Lee, B.P., Messersmith, P.B., 2007. A reversible wet/dry adhesive inspired by mussels and geckos. Nature 448, 338–341. https://doi.org/10.1038/nature05968.

Lee, M., Zhang, W., Noll, B.C., 2009. Total Synthesis of Sporolide B. Angew. Chemie Int. Ed. 48, 3449–3453. https://doi.org/10.1002/anie.200900264.

Li, J.J., Johnson, D.S., Sliskovic, D.R., Roth, B.D., 2004. Contemporary Drug Synthesis. John Wiley & Sons, Inc., Hoboken, New Jersey.

Li, L., Li, Y., Luo, X., Deng, J., Yang, W., 2010. Helical poly(N-propargylamide)s with functional catechol groups: Synthesis and adsorption of metal ions in aqueous solution. React. Funct. Polym. 70, 938–943. https://doi.org/10.1016/j.reactfunctpolym.2010.09.006.

Liu, M., Ji, J., Zhang, X., Zhang, X., Yang, B., Deng, F., Zhen Li, Z., Wang, K., Yang, Y., Wei, Y., 2015. Self-polymerization of dopamine and polyethyleneimine: novel fluorescent organic nanoprobes for biological imaging applications. J. Mater. Chem. B 3, 3476–3482. https://doi.org/10.1039/C4TB02067G.

Liu, M., Zeng, G., Wang, K., Wan, Q., Tao, L., Zhang, X., Wei, Y., 2016. Recent developments in polydopamine: an emerging soft matter for surface modification and biomedical applications. Nanoscale 8, 16819–16840. https://doi.org/10.1039/C5NR09078D.

Ly, H.B., Poupart, R., Carbonnier, B., Monchiet, V., Le Droumaguet, B., Grande, D., 2017. Versatile functionalization platform of biporous poly(2-hydroxyethyl methacrylate)-based materials: Application in heterogeneous supported catalysis. React. Funct. Polym. 121, 91–100. https://doi.org/10.1016/j.reactfunctpolym.2017.10.024.

Morinaga, H., Ochiai, B., Endo, T., 2007. Metal-free ring-opening polymerization of glycidyl phenyl ether by tetrabutylammonium fluoride. Macromolecules 40, 6014–6016. https://doi.org/10.1021/MA070386Z.

Morinaga, H., Ujihara, Y., Yamanaka, T., Nagai, D., Endo, T., 2011a. Metal-free ring-opening polymerization of glycidyl phenyl ether initiated by tetra-n-butylammonium acetate and its application to the hydroxyl-terminated telechelic polymer. J. Polym. Sci. Part A Polym. Chem. 49, 4092–4097. https://doi.org/10.1002/pola.24833.

Morinaga, H., Ujihara, Y., Yuto, N., Nagai, D., Endo, T., 2011b. Controlled polymerization of epoxides: Metal-free ring-opening polymerization of glycidyl phenyl ether initiated by tetra-n-butylammonium fluoride in the presence of protic compounds. J. Polym. Sci. Part A Polym. Chem. 49, 5210–5216. https://doi.org/10.1002/pola.24990.

Nelson, S.D., Omichinski, J.G., Iyer, L., Gordon, W.P.P., Soderlund, E.J., Dybing, E., 1984. Activation mechanism of Tris(2,3-dibromopropyl)phosphate to the potent mutagen, 2-bromoacrolein. Biochem. Biophys. Res. Commun. 121, 213–219. https://doi.org/10.1016/0006-291X(84)90709-5.

Nicolaou, K.C., Wang, J., Tang, Y., Botta, L., 2010. Total synthesis of sporolide B and 9-epi-sporolide B. J. Am. Chem. Soc. 132, 11350–11363. https://doi.org/10.1021/ja1048994.

Pan, X.D., Qin, Z., Yan, Y.Y., Sadhukhan, P., 2010. Elastomers with chain-end mussel-mimetic modification for nanocomposites: Strong modifications to reinforcement and viscoelastic properties. Polymer (Guildf). 51, 3453–3461. https://doi.org/10.1016/j.polymer.2010.05.031.

Quirk, R.P., Lizarraga, G.M., 2000. Anionic synthesis of well-defined, poly[(styrene)-block-(propylene oxide)] block copolymers. Macromol. Chem. Phys. 201, 1395–1404. https://doi.org/10.1002/1521-3935(20000801)201:13<1395::AID-MACP1395>3.0.CO;2-H.

Sakakibara, K., Nakano, K., Nozaki, K., 2007. Regioregular polymerization of fluorine-containing epoxides. Macromolecules 40, 6136–6142. https://doi.org/10.1021/ma070428j.

Sakakibara, K., Nakano, K., Nozaki, K., 2006. Regio-controlled ring-opening polymerization of perfluoroalkyl-substituted epoxides. Chem. Commun. 57, 3334. https://doi.org/10.1039/b606693c.

Sarazin, Y., Carpentier, J.-F., 2015. Discrete cationic complexes for ring-opening polymerization catalysis of cyclic esters and epoxides. Chem. Rev. 115, 3564–3614. https://doi.org/10.1021/acs.chemrev.5b00033.

Shao, H., Stewart, R.J., 2010. Biomimetic underwater adhesives with environmentally triggered setting mechanisms. Adv. Mater. 22, 729–733. https://doi.org/10.1002/adma.200902380.

Shi, Y., Jiang, R., Liu, M., Fuc, L., Zeng, G., Wan, Q., Mao, L., Deng, F., Zhang, X., Wei, Y., 2017. Facile synthesis of polymeric fluorescent organic nanoparticles based on the self-polymerization of dopamine for biological imaging. Mater. Sci. Eng. C 77, 972–977. https://doi.org/10.1016/j.msec.2017.04.033.

Tian, Y., Cao, Y., Wang, Y., Yang, W., Feng, J., 2013. Realizing ultrahigh modulus and high strength of macroscopic graphene oxide papers through crosslinking of mussel-inspired polymers. Adv. Mater. 25, 2980–2983. https://doi.org/10.1002/adma.201300118.

Toshiko, O., 1991. Sesamol and sesaminol as antioxidants. New Food Ind. 33, 1–5.

Wagner, S., Kopka, K., Law, M.P., Riemann, B., Pike, V.W., Schober, O., Schäfers, M., 2004. Synthesis and first in vivo evaluation of new selective high affinity β1-adrenoceptor radioligands for SPECT based on ICI 89,406. Bioorg. Med. Chem. 12, 4117–4132. https://doi.org/10.1016/j.bmc.2004.05.027.

Wang, Z., Duan, Y., Duan, Y., 2018. Application of polydopamine in tumor targeted drug delivery system and its drug release behavior. J. Control. Release 290, 56–74. https://doi.org/10.1016/j.jconrel.2018.10.009.

Wynn, J.P., Kendrick, A., Ratledge, C., 1997. Sesamol as an inhibitor of growth and lipid metabolism in Mucor circinelloides via its action on malic enzyme. Lipids 32, 605–610. https://doi.org/10.1007/s11745-997-0077-1.

Yang, H.-C., Luo, J., Lv, Y., Shen, P., Xu, Z.-K., 2015. Surface engineering of polymer membranes via mussel-inspired chemistry. J. Memb. Sci. 483, 42–59. https://doi.org/10.1016/j.memsci.2015.02.027.

Zeng, G., Huang, L., Huang, Q., Liu, M., Xu, D., Huang, H., Yang, Z., Deng, F., Zhang, X., Wei, Y., 2018. Rapid synthesis of MoS_2-PDA-Ag nanocomposites as heterogeneous catalysts and antimicrobial agents via microwave irradiation. Appl. Surf. Sci. 459, 588–595. https://doi.org/10.1016/j.apsusc.2018.07.144.

Zhang, F., Liu, S., Zhang, Y., Wei, Y., Xu, J., 2012. Underwater bonding strength of marine mussel-inspired polymers containing DOPA-like units with amino groups. RSC Adv. 2, 8919–8921. https://doi.org/10.1039/C2RA21312E.

Zhang, K., Zhang, F., Song, Y., Fan, J.-B., Wang, S., 2017a. Recent progress of mussel-inspired underwater adhesives. Chinese J. Chem. 35, 811–820. https://doi.org/10.1002/cjoc.201600778.

Zhang, X., Huang, Q., Deng, F., Huang, H., Wan, Q., Liua, M., Wei, Y., 2017b. Mussel-inspired fabrication of functional materials and their environmental applications: Progress and prospects. Appl. Mater. Today 7, 222–238. https://doi.org/10.1016/j.apmt.2017.04.001.

Zhao, H., Sun, C., Stewart, R.J., Waite, J.H., 2005. Cement proteins of the tube-building polychaete Phragmatopoma californica. J. Biol. Chem. 280, 42938–42944. https://doi.org/10.1074/jbc.M508457200.